Infrared Spectra of Mass-Selected Mg^+-H_2 and Mg^+-D_2 Complexes

Viktoras Dryza, Berwyck L. Poad, and Evan J. Bieske*

School of Chemistry, The University of Melbourne, Victoria, 3010, Australia

Received: October 6, 2008

Rotationally resolved infrared spectra of Mg^+-H_2 and Mg^+-D_2 are recorded in the H−H (4025−4080 cm^{-1}) and D−D (2895−2945 cm^{-1}) stretch regions by monitoring Mg^+ photofragments. The ν_{HH} and ν_{DD} transitions of Mg^+-H_2 and Mg^+-D_2 are red-shifted by 106.2 ± 1.5 and 76.0 ± 0.1 cm^{-1} respectively from the fundamental vibrational transitions of the free H_2 and D_2 molecules. The spectra are consistent with a T-shaped equilibrium structure in which the Mg^+ ion interacts with a slightly perturbed H_2 or D_2 molecule. From the spectroscopic constants, a vibrationally averaged intermolecular separation of 2.716 Å (2.687 Å) is deduced for the ground state of Mg^+-H_2 (Mg^+-D_2), decreasing by 0.037 Å (0.026 Å) when the H_2 (D_2) subunit is vibrationally excited.

1. Introduction

Interactions between metal cations and neutral molecules play key roles in a variety of contexts including gas storage in solid materials, ion solvation, laser plasmas, and atmospheric and astrophysical processes. One route for characterizing the interactions between metal cations (M^+) and neutral molecules (L) is to form and spectroscopically probe M^+-L_n complexes in the gas phase. Complexes containing the magnesium cation have played an important role in this program. The studies, which have embraced Mg^+ attached to Ar, H_2 O, D_2, N_2, CO_2, CH_4, CH_2O, and pyridine, have usually entailed exciting the $^2P \leftarrow {}^2S$ electronic transitions centered on the Mg^+ ion.[1−5] Recently, complexes such as $Mg^+-(H_2O)_n$ have also been probed through their infrared absorptions in the O−H stretch region.[6]

In this paper, spectroscopic studies of charged complexes containing the magnesium cation are extended to include Mg^+-H_2 and Mg^+-D_2, which are probed by using infrared (IR) photodissociation spectroscopy in the H−H and D−D stretch regions, respectively. The resulting spectra feature full rotational resolution giving access to vibrationally averaged intermolecular bond lengths, the H−H and D−D stretch vibrational frequencies, and estimates for the intermolecular stretch vibrational frequencies. The ensuing data should serve to test potential energy surfaces for the $Mg^+\cdots H_2$ interaction and complement recent spectroscopic and theoretical investigations of other metal cation−dihydrogen complexes including Li^+-H_2, Al^+-H_2, B^+-H_2, and Na^+-H_2.[7−11]

A more comprehensive understanding of the interaction between Mg^+ and H_2 is desirable for several reasons. Perhaps most important are insights into hydrogen storage materials containing magnesium, including metal hydrides,[12,13] metal−organic frameworks,[14,15] and metal cation-doped zeolites.[16,17] Areán and co-workers have examined H_2 absorption in a magnesium-containing zeolite using variable-temperature FTIR spectroscopy.[16] By monitoring the intensity of the H−H stretch vibrational band associated with H_2 attached to the Mg^{2+} sites (4056 cm^{-1}), the standard enthalpy of H_2 adsorption was found to be −18.2 kJ/mol, considerably higher in magnitude than that for Li^+ and Na^+ sites in zeolites. The binding energy is, however, far lower than that for the interaction between Mg^{2+} and H_2 in the gas phase for which calculations give values closer to −92 kJ/mol.[18,19] Although the formal charge of Mg ions in the zeolites is 2+, charge transfer from the surrounding framework inevitably reduces the effective charge and magnitude of the adsorption enthalpy.

In the only previous spectroscopic investigation, the electronic transitions of Mg^+-D_2 were probed over the 280−315 nm range by monitoring MgD^+ photofragments.[2,20] The spectrum displayed a long vibrational progression associated with the $^2B_1 \leftarrow {}^2A_1$ transition superimposed on a broad continuum background associated with the $^2B_2 \leftarrow {}^2A_1$ transition. The vibrational progression, which exhibited an interval that decreased from 489 to 314 cm^{-1}, was assigned to the intermolecular stretch in the $^2B_1$ state. Overall, the spectral features were quite broad making it difficult to derive detailed structural information. In recent related work, reactions between laser-cooled Mg^+ ions in the excited 3p state and H_2, D_2, and HD molecules have been investigated.[21] Intriguingly, reactions between Mg^+ and HD preferentially produce MgD^+ rather than MgH^+. The Mg^+-H_2 complex has also been considered as a possible constituent of the interstellar medium with Petrie and Dunbar concluding that radiative association of Mg^+ and H_2 proceeds too slowly for the formation of appreciable Mg^+-H_2 abundances.[22]

There have been several ab initio studies of Mg^+-H_2 giving disparate structural parameters. Originally, HF/6-31G* level calculations by Curtiss and Pople predicted that Mg^+-H_2 is a T-shaped, C_{2v} complex with a relatively long $Mg^+\cdots H_2$ intermolecular bond (3.73 Å), and a binding energy of 200 cm^{-1}.[23] Later, more reliable CASSCF calculations by Bauschlicher confirmed the T-shaped structure but suggested a much shorter intermolecular bond of 2.72 Å, a dissociation energy of 525 cm^{-1}, and an H−H bond that is 0.006 Å longer than that of the free H_2 molecule.[24] Subsequently, Petrie and Dunbar reported rotational constants determined at the MP2(full)/6-31G* level that are compatible with an intermolecular bond length of 3.48 Å. Spectroscopic investigations described in this paper provide empirical values for the intermolecular separation and intermolecular stretch vibrational frequency allowing a critical assessment of the earlier calculations.

* Corresponding author. E-mail: evanjb@unimelb.edu.au.

10.1021/jp808807r CCC: $40.75
Published on Web 12/10/2008

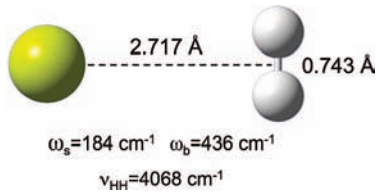

Figure 1. Geometrical parameters and vibrational frequencies for Mg^+-H_2 calculated at the MP2/aug-cc-pVTZ level. Note that the H−H stretch frequency has been scaled by 0.921 (see Section 2).

2. Experimental and Theoretical Approaches

Infrared spectra of $^{24}Mg^+-H_2$ and $^{24}Mg^+-D_2$ were obtained by monitoring $^{24}Mg^+$ photodissociation products while scanning the IR wavelength over the H−H or D−D stretch region. The complexes were generated in a supersonic expansion of H_2 or D_2 (8 bar) passed over a laser-ablated magnesium rod. The translating/rotating rod was irradiated with the fundamental (1064 nm, 7 mJ/pulse), doubled (532 nm, 3 mJ/pulse), and quadrupled (266 nm, 1 mJ/pulse) output of a pulsed Nd:YAG laser running at 20 Hz. The Mg^+-H_2 and Mg^+-D_2 complexes were mass-selected by a quadrupole mass filter and deflected through 90° by a quadrupole bender into an octopole ion guide where they were overlapped by the counterpropagating output of a pulsed, tunable IR optical parametric oscillator (Continuum Mirage 3000, bandwidth of 0.017 cm^{-1}). The Mg^+ photofragments were mass-selected by a second quadrupole mass filter and detected by using a microchannel plate coupled to a scintillator and a photomultiplier tube. The observed transition intensities were not normalized for laser power or parent ion flux (which exhibits shot-to-shot and longer term fluctuations). Spectral calibration was achieved by using previously described methods.[7] The absolute uncertainty of the line wavenumbers is decided by the uncertainty of the ion energy in the octopole ion guide and is estimated as ±0.10 cm^{-1}.

One difficulty associated with recording the $^{24}Mg^+-H_2$ spectrum stems from the presence of isobaric $^{26}Mg^+$ ions (11% natural abundance) which are present in far higher abundance than the target complex. Slight transmission of $^{26}Mg^+$ ions through the second quadrupole mass filter leads to an appreciable background signal that degrades the $^{24}Mg^+-H_2$ spectrum. This problem does not occur for $^{24}Mg^+-D_2$ and consequently the signal-to-noise ratio of the $^{24}Mg^+-D_2$ spectrum is somewhat better than that of the $^{24}Mg^+-H_2$ spectrum.

Ab initio calculations for Mg^+-H_2 were carried out by using the MP2 method with the Dunning aug-cc-pVTZ basis set and employed the Gaussian 03 suite of programs.[25] The dissociation energy for Mg^+-H_2 was calculated taking into account harmonic zero-point energies but ignoring basis set superposition error. The calculated H−H stretch vibrational frequency was scaled by the factor required to reconcile the calculated and experimental frequencies for the free H_2 molecule (0.921).

3. Results

3.1. Mg^+-H_2. The calculated equilibrium structure and harmonic vibrational frequencies of Mg^+-H_2 are shown in Figure 1. In accordance with previous theoretical studies, Mg^+-H_2 is predicted to have a T-shaped, C_{2v} equilibrium structure with the Mg^+ ion attached to a weakly perturbed H_2 molecule.

The energy levels of the Mg^+-H_2 complex in the $^2A_1$ ground electronic state can be labeled by using quantum numbers appropriate for a doublet, near-prolate, asymmetric rotor (J, N, K_a, and K_c). For Hund's Case (b) coupling, the total angular momentum excluding nuclear spin ($\hat{J}$) is related to the rotational angular momentum ($\hat{N}$) and the total electronic spin ($\hat{S}$) by $\hat{J} = \hat{N} + \hat{S}$. The quantum numbers K_a and K_c describe the projections of the rotational angular momentum along the a and c axes in the prolate and oblate top limits, respectively. For the Mg^+-H_2 complex, the a-axis corresponds to the intermolecular axis.

Each rotational N value is associated with $J = N - {}^1/_2$ and $J = N + {}^1/_2$ sublevels that are separated due to coupling between the electronic spin and molecular rotation. The MP2/aug-cc-pVTZ ab initio calculations for Mg^+-H_2 suggest that the electronic spin-rotation splitting is small (predicted constants are $\epsilon_{aa} = -1.34 \times 10^{-3}$ cm^{-1}, $\epsilon_{bb} = 1.2 \times 10^{-4}$ cm^{-1}, and $\epsilon_{cc} = 1.0 \times 10^{-4}$ cm^{-1}) and indeed we are unable to resolve spin-rotation splitting in the Mg^+-H_2 and Mg^+-D_2 infrared spectra. Therefore, spin-rotation coupling is disregarded in the subsequent analysis and the energy levels are labeled only with the quantum numbers N, K_a, and K_c.

Because the transition moment associated with excitation of the H−H stretch lies along the a-axis, the infrared transitions of Mg^+-H_2 are characteristic of a parallel A-type transition and follow $\Delta K_a = 0$ and $\Delta K_c = \pm 1$ selection rules. For transitions originating from $K_a = 0$ and $K_a \geq 1$ states, the total angular momentum selection rules are $\Delta J = \pm 1$ and $\Delta J = 0, \pm 1$, respectively. Selection rules for N are identical with those for J.

The infrared spectrum of Mg^+-H_2 over the 4025−4080 cm^{-1} range is shown in Figure 2. The spectrum exhibits well-resolved rovibrational features belonging to the $K_a = 1-1$ sub-band, associated with complexes containing the ortho form of H_2 (odd j levels). There is no trace of the $K_a = 0-0$ sub-band associated with complexes containing para H_2 (even j levels). A similar preponderance of complexes containing ortho H_2 has been observed for other neutral and charged complexes[9,26,27] and, in part, reflects the 1:3 para/ortho population ratio in normal hydrogen gas. Furthermore, a free H_2 molecule in the $j = 1$ state has ~120 cm^{-1} more rotational energy than a $j = 0$ H_2 molecule; this rotational energy is partially quenched in the complex leading to a stabilization of Mg^+-H_2 (ortho) relative to Mg^+-H_2 (para). Therefore, Mg^+-H_2 (para) complexes are likely to be converted to the more stable Mg^+-H_2 (ortho) complexes in the ion source through rapid, exothermic, ligand switching reactions.

Altogether, 38 transitions were assigned to the $K_a = 1-1$ sub-band (22 P-branch and 16 R-branch lines), with asymmetry doublets resolved in the P and R branches. The Q-branch lines were overlapped and were excluded from the fit. Transition wavenumbers and assignments are provided as Supporting Information. The $K_a = 1-1$ transitions of Mg^+-H_2 were fitted by using an A-reduced Watson Hamiltonian with adjustable parameters including the ground and excited state B, C, and Δ_J rotational constants. It is not possible to determine the ground and excited state A rotational constants through analysis of the parallel transition. Therefore for the fit, A'' and A' were constrained to 59.34 cm^{-1}, the rotational constant of free H_2 in the $n_{HH} = 0$ state.[28] Note that the fits are insensitive to the absolute values of A'' and A'; virtually identical B, C, and Δ_J values are obtained for A'' and A' ranging from 50 to 70 cm^{-1}. Resulting spectroscopic constants for Mg^+-H_2 are listed in Table 1.

Because no $K_a = 0-0$ transitions were observed for Mg^+-H_2, the ν_{HH} band center cannot be determined directly. However, it is estimated to lie between Δb and $2\Delta b$ above the $K_a = 1-1$ sub-band center (4050.5 cm^{-1}). Here, $\Delta b \approx 3$ cm^{-1} is the difference in the H_2 rotational constant in the $n_{HH} = 0$ and 1

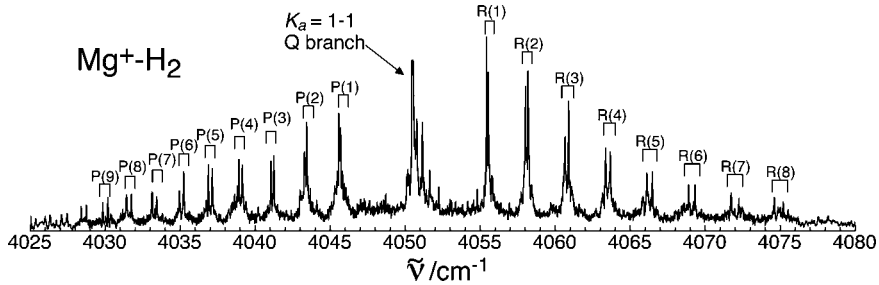

Figure 2. Infrared spectrum of $^{24}Mg^+-H_2$ in the H−H stretch region obtained by monitoring Mg^+ photofragments. The $K_a = 1-1$ P, Q, and R branch transitions are labeled.

TABLE 1: Spectroscopic Constants (in cm^{-1} unless otherwise indicated) for $^{24}Mg^+-H_2$ and $^{24}Mg^+-D_2$ Obtained by Fitting the ν_{HH} and ν_{DD} Transitions to a Watson *A*-Reduced Hamiltonian[a]

	Mg^+-H_2	Mg^+-D_2			
	K_a=1−1	K_a=0−0	K_a=1−1	K_a=2−2	K_a=0−0,1−1
B''	1.2411(14)		0.6807(11)		0.6804(11)
C''	1.1916(14)		0.6587(11)		0.6584(11)
$\overline{B}''$	1.2164(14)	0.6708(12)	0.6697(11)	0.6679(14)	0.6694(11)
$\Delta''_J \times 10^4$	1.925(42)	0.57(4)	0.527(32)	0.540(40)	0.514(20)
$\Delta''_{JK} \times 10^4$					−1.39(49)
B'	1.2762(14)		0.6941(11)		0.6937(11)
C'	1.2233(14)		0.6708(11)		0.6705(11)
$\overline{B}'$	1.2498(14)	0.6836(12)	0.6824(11)	0.6799(14)	0.6821(11)
$\Delta'_J \times 10^4$	1.751(51)	0.53(4)	0.503(32)	0.492(36)	0.471(23)
$\Delta''_{JK} \times 10^4$					−3.14(39)
ΔA					1.464(12)
ν_{sub}	4050.46(1)	2917.56(2)	2916.09(1)	2912.05(2)	2917.55(1)
rms × 10^3	4.8	3.5	7.6	2.6	10.5
$\Delta\nu_{HH}$	−106.2(1.5)				−76.0(0)
ω''_s	193				153
ω'_s	211				164
R''_0 /Å	2.716				2.687
R'_0 /Å	2.679				2.661

[a] For each value, the error in the last significant figure(s) is given in parentheses.

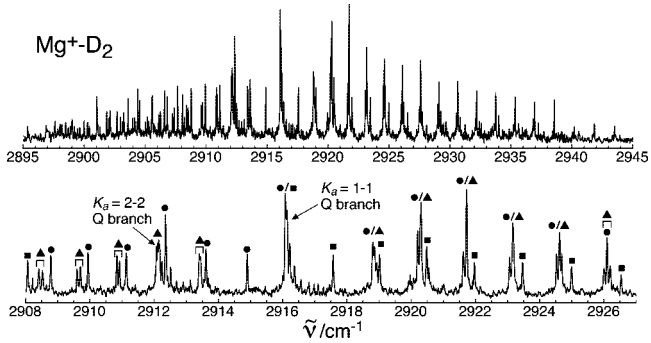

Figure 3. Top: Infrared spectrum of $^{24}Mg^+-D_2$ in the D−D stretch region obtained by monitoring Mg^+ photofragments. Bottom: Expanded central region of the Mg^+-D_2 spectrum. The $K_a = 0-0$ (circles), 1−1 (triangles), and 2−2 (squares) transitions are labeled.

states, and the lower and upper limits are based on the Mg^+-H_2 complex being a rigid prolate rotor or containing a freely rotating hydrogen subunit, respectively. For the moment, the band center is deemed as the average of the lower and upper limits (i.e., 4055.0 cm^{-1}). This corresponds to a red-shift of 106.2 cm^{-1} with respect to the $Q_1(0)$ transition of the free H_2 molecule (4161.2 cm^{-1}).[29]

3.2. Mg^+-D_2. The infrared spectrum of Mg^+-D_2 over the 2895−2945 cm^{-1} range is shown in Figure 3. Many more transitions are observed for Mg^+-D_2 than for Mg^+-H_2, with $K_a = 0-0$, 1−,1 and 2−2 transitions all appearing in the spectrum. The presence of the $K_a = 0$ and 2 complexes in detectable abundances for Mg^+-D_2 but not for Mg^+-H_2 is a consequence of a better signal-to-noise ratio of the Mg^+-D_2 spectrum (see Section 2), the fact that the population ratio of even to odd j levels in D_2 is 2:1 rather than 1:3 in H_2, and because the ligand switching reaction which favors the $K_a = 1$ complexes is less exothermic for D_2 than for H_2. Altogether, 79 transitions were assigned to the $K_a = 0-0$ (14 P-branch and 14 R-branch lines), $K_a = 1-1$ (18 P-branch and 20 R-branch lines), and $K_a = 2-2$ (6 P-branch and 7 R-branch lines) sub-bands. Asymmetry doublets were resolved in the P and R branches of the $K_a = 1-1$ sub-band, but not the $K_a = 2-2$ sub-band.

As described above for Mg^+-H_2, the transitions of Mg^+-D_2 were fitted by using an *A*-reduced Watson Hamiltonian. For fitting the sub-bands individually, A'' and A' were constrained to 29.907 cm^{-1}, the ground state rotational constant of the free D_2 molecule.[28] When two or more sub-bands were fitted together, A'' was constrained to 29.907 cm^{-1} while A' was allowed to vary. The fit of a parallel transition can only yield $\Delta A = A' - A''$ and is relatively insensitive to the absolute values of A'' and A'. A reasonable fit was obtained for the $K_a = 0-0$ and 1−1 sub-bands together (rms = 1.0×10^{-2} cm^{-1}); however the fit deteriorated when the $K_a = 2-2$ transitions were also included (rms = 4.2×10^{-2} cm^{-1}), despite the latter sub-band giving a good fit by itself. The difficulty in fitting simultaneously the $K_a = 0-0$, 1−1, 2−2 transitions by using a limited number of adjustable parameters is presumably a consequence of the large-amplitude bending motion of the floppy complex. Resulting spectroscopic constants for Mg^+-D_2 are listed in Table 1.

TABLE 2: Calculated and measured properties of $^{24}Mg^+-H_2$

	exptl[1]	MP2/ aug-cc-pVTZ[a]	CASSCF[b]	MP2(full)/ 6-31G* [c]
ω_s/cm^{-1}	193	184	180	69
ω_b/cm^{-1}		436	410	124
$\Delta\nu_{HH}/cm^{-1}$	−106.2	−93	−85	
R_e/Å		2.72	2.72	3.48
R_0/Å	2.716			
D_0/Å		416	525	485

[a] Current work. [b] Reference 30. $\Delta\nu_{HH}$ is based on a scaled ν_{HH} frequency (scaling factor = 0.945). [c] Reference 22.

Transition wavenumbers and assignments are provided as Supporting Information.

The ν_{DD} transition for Mg^+-D_2 occurs at 2917.6 cm^{-1} corresponding to a shift of $\Delta\nu_{DD} = -76.0$ cm^{-1} from the $Q_1(0)$ transition of the free D_2 molecule (2993.6 cm^{-1}). The ratio of the Mg^+-H_2 and Mg^+-D_2 shifts $\Delta\nu_{HH}/\Delta\nu_{DD} = 1.40$ is close to the ratio expected if the H−H and D-D stretch modes are decoupled from the remaining vibrational modes ($\Delta\nu_{HH}/\Delta\nu_{DD} = (m_D/m_H)^{1/2} = 1.41$).

4. Discussion

4.1. Structural, Energetic, and Vibrational Properties. Overall, the spectroscopic data confirm that Mg^+-H_2 is a T-shaped complex consisting of a Mg^+ ion attached to a slightly perturbed H_2 molecule by charge-quadrupole electrostatic and charge-induced-dipole induction interactions. Evidence for the weak nature of the intermolecular bond is that the H_2 vibrational frequency is reduced by only 2.6% and that the vibrationally averaged intermolecular bond length deduced from the *B* and *C* rotational constants (2.716 Å) is typical for complexes of this type.[18] Generally, the properties of Mg^+-D_2 are similar to those of Mg^+-H_2 although it possesses a slightly shorter vibrationally averaged intermolecular bond (by 0.029 Å), presumably due to reduced zero-point vibrational motion in the intermolecular stretch coordinate. The intermolecular bonds of Mg^+-H_2 and Mg^+-D_2 shorten upon vibrational excitation of the diatomic subunit (by 0.037 and 0.026 Å, respectively); this can be seen as a consequence of enhancements to the electrostatic and induction interactions following increases in the quadrupole moments and polarizabilities of H_2 and D_2 in their excited vibrational states.

Unfortunately, the Mg^+-H_2 and Mg^+-D_2 infrared spectra provide no information on the H−H and D−D bond distances. For a completely rigid T-shaped complex it is possible to deduce the *A* rotational constant and therefore the H−H separation from *B* and *C* as the inertial defect $\Delta = 1/C - 1/B - 1/A$ is zero. However, the large-amplitude zero-point bending motion in Mg^+-H_2 leads to an exaggeration of the asymmetry spitting and a nonzero inertial defect rendering it impossible to deduce *A*.[26,31] However, on the basis of the MP2/aug-cc-pVTZ calculations, the H−H bond is predicted to lengthen by 0.006 Å compared to the free H_2 molecule (0.737 Å).

Measured and calculated structural and vibrational properties of Mg^+-H_2 are summarized in Table 2. Generally, the measured properties are consistent with the MP2/aug-cc-pVTZ results and the earlier CASSCF calculations of Bauschlicher, with good agreement for the vibrational red-shift $\Delta\nu_{HH}$, the harmonic intermolecular stretch frequency (ω_s), and the intermolecular separation. The Mg^+-H_2 vibrationally averaged intermolecular separation R_0 =2.716 Å agrees very well with the R_e = 2.717 Å equilibrium separation determined from the MP2/aug-cc-pVTZ calculations (see Figure 1). To some extent, the agreement is probably fortuitous as one would expect the vibrationally averaged intermolecular separation to exceed slightly the equilibrium separation. In contrast, the MP2(full)/6-31G* level calculations described in ref 22 severely overestimate the intermolecular bond length (by 0.8 Å) and underestimate the intermolecular stretch frequency (by ∼120 cm^{-1}). Apparently, the 6-31G* basis set is too small to provide an adequate structural description of Mg^+-H_2. Despite this, the MP2(full)/6-31G* binding energy (D_0 =485 cm^{-1}) agrees reasonably well with the MP2/aug-cc-pVTZ and CASSCF values (D_0 =416 and 525 cm^{-1}, respectively).

The Mg^+-H_2 and Mg^+-D_2 spectra furnish little direct information on the frequencies of the intermolecular stretch and bend vibrational modes (ν_s and ν_b) as the $\nu_{HH} + \nu_s$ and $\nu_{HH} + \nu_b$ combination bands have not been observed. However, the harmonic intermolecular stretch frequency of Mg^+-H_2, estimated from the $\overline{B}$ and Δ_J rotational constants (ω_s =193 cm^{-1}), is close to the calculated MP2/aug-cc-pVTZ value (184 cm^{-1}). For Mg^+-D_2, the harmonic intermolecular stretch frequency estimated from $\overline{B}$ and Δ_J is 153 cm^{-1}. In a pseudodiatomic approximation the ω_s values for Mg^+-D_2 and Mg^+-H_2 should have a ratio of 0.73, which is close to the ratio estimated from the spectroscopic constants (0.79).

The bending mode harmonic frequencies derived from MP2/aug-cc-pVTZ and CASSCF calculations are similar (436 and 410 cm^{-1}, respectively). However, the actual bending frequency is certainly somewhat lower considering that the barrier for internal rotation of the H_2 subunit is only 380 cm^{-1} (at the MP2/aug-cc-pVTZ level). Ultimately, a more comprehensive understanding of the large-amplitude intermolecular vibrations of Mg^+-H_2 must await rovibrational energy level calculations using a full three-dimensional potential energy surface. These calculations will also allow a more rigorous comparison between the measured and computed rotational constants for the Mg^+-H_2 and Mg^+-D_2 complexes.

4.2. Vibrational Predissociation Dynamics. The observed IR transitions of Mg^+-H_2 access quasibound $n_{HH} = 1$ levels that are coupled to the $Mg^+ + H_2$ ($n_{HH} = 0$) continuum. In principle, the vibrational predissociation rate can be extracted from the widths of the individual rovibrational lines. Broadening due to unresolved spin-rotation structure is expected to be negligible compared to the band width of the excitation light. Several of the more intense Mg^+-H_2 $K_a = 1-1$ lines were used to estimate the lifetime broadening by fitting them to a Voigt profile with the full width half-maximum of the Gaussian component fixed to 0.017 cm^{-1} (the bandwidth of the OPO IR radiation). The width of the resulting Lorentzian component is 0.045 ± 0.005 cm^{-1}, corresponding to an upper state lifetime of τ_{vp} =120 ps. For Mg^+-D_2, the width of the Lorentzian component for several of the more intense $K_a = 0-0$ lines is 0.030 ± 0.002 cm^{-1}, corresponding to an upper state lifetime of τ_{vp} =180 ps. These τ_{vp} values should be taken as provisional lower limits as the lines may be power broadened or Doppler broadened due to the ions having a spread of energy in the octopole region where they overlap with IR radiation. It should be noted that using the same instrument we have observed narrower, laser-limited transitions for Br^--D_2 and I^--D_2.[32,33]

4.3. Comparisons with Related Complexes. It is interesting to compare the properties of Mg^+-H_2 and other similar metal cation−H_2 complexes. As expected, the intermolecular bond length of Mg^+-H_2 (2.716 Å) exceeds that of Na^+-H_2 (2.493 Å) but is less than that of Al^+-H_2 (3.035 Å); the bond length ordering reflects the Pauli repulsion between the H_2 σ_g orbital

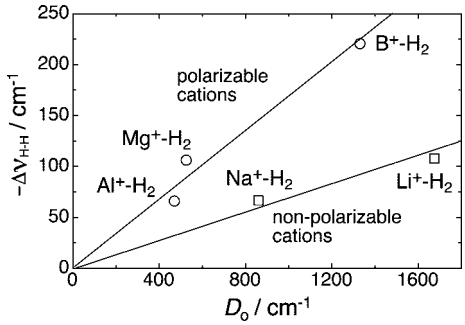

Figure 4. H−H stretch vibrational frequency shift ($-\Delta\nu_{HH}$) plotted against dissociation energy (D_0) for Li^+-H_2, B^+-H_2, Na^+-H_2, Mg^+-H_2, and Al^+-H_2. Trendlines are shown for complexes containing polarizable metal cations (○) and nonpolarizable metal cations (□). The plotted data are experimental values apart from the D_0 values of Li^+-H_2 and Mg^+-H_2, which are calculated values taken from refs 40 and 24, respectively.

and the half-filled and filled 3 s orbital in Mg^+ and Al^+, respectively.[34] Similarly, one might anticipate that the binding energy of Mg^+-H_2 should be bracketed by the binding energies of Na^+-H_2 and Al^+-H_2 (measured as 860 and 470 cm^{-1}, respectively; refs 35 and 36). Direct comparisons are difficult because the binding energy of Mg^+-H_2 has not been measured. The calculated MP2/aug-cc-pVTZ Mg^+-H_2 binding energy (D_0 = 420 cm^{-1}) lies below the expected range, although it should be noted that this computational approach tends to underestimate the dissociation energies of M^+-H_2 complexes by 100−200 cm^{-1}.[35−37] The CASSCF calculations of Bauschlicher predict a somewhat higher binding energy (525 cm^{-1}), according better with expectations.[24]

The ν_{HH} red-shift for complexes containing H_2 is often presumed to be connected directly with the dissociation energy.[38,39] From this perspective, it is interesting to compare the vibrational red-shift ($\Delta\nu_{HH}$) and binding energy (D_0) for Mg^+-H_2 with those of the Li^+-H_2, Na^+-H_2, B^+-H_2, and Al^+-H_2 complexes which have also been characterized spectroscopically.[10] Interestingly, when $\Delta\nu_{HH}$ is plotted against D_0 (see Figure 4), the data for complexes containing cations with a half-filled or filled valence s orbital (B^+, Mg^+, Al^+) and the data for complexes containing alkali metal cations (Li^+, Na^+) lie on two separate lines. Generally, complexes containing the polarizable B^+, Mg^+, and Al^+ cations exhibit a larger ν_{HH} red-shift for a given dissociation energy than complexes containing the nonpolarizable Li^+ and Na^+ cations. The differences are highlighted by comparing Mg^+-H_2 and Li^+-H_2. The $\Delta\nu_{HH}$ value for Mg^+-H_2 (−106.2 cm^{-1}) is similar to that of Li^+-H_2 (−107.8 cm^{-1}) yet Mg^+-H_2 has a much lower dissociation energy (525 cm^{-1} compared to 1675 cm^{-1}; refs 24 and 40) and a considerably longer intermolecular bond (2.703 Å compared to 2.056 Å; ref 8).

Reasons for the larger than expected red-shifts for complexes containing metal cations with a single or doubly occupied valence s orbital were elaborated in our previous study of the B^+-H_2 complex.[10] It was found that a small admixture of the B^+ 2 p_z orbital in the HOMO (primarily B^+ 2 s and H_2 σ_g in character) results in electron density transfer from the H_2 σ_g orbital (0.02 electrons) to the 2 p_z orbital causing the pronounced reduction of the ν_{HH} frequency (i.e., a large red-shift). Involvement of the 2 p_z orbital is promoted by polarization of the valence 2 s orbital away from the H_2 molecule by electrons in the σ_g orbital. A similar effect is likely to occur for Mg^+-H_2 (with transfer from the σ_g bonding orbital to the Mg^+ 3 p_z orbital). In contrast, for Li^+-H_2 and Na^+-H_2 complexes, the alkali metal's unoccupied s and p orbitals lie much higher in energy and do not effectively hybridize with the σ_g orbital.

Polarization of the filled or half-filled valence s orbital of a metal cation by attached ligands plays an important role in deciding the structures of the larger $M^+-(H_2)_n$ complexes. The $B^+-(H_2)_2$, $Al^+-(H_2)_2$, and $Mg^+-(H_2)_2$ species are all predicted to have bent structures; two H_2 ligands positioned on the same side of the metal ion can concertedly polarize the cation allowing their closer approach to the positively charged core.[34,36,41] In contrast, the $Li^+-(H_2)_2$ and $Na^+-(H_2)_2$ species are predicted to be linear, with the two H_2 ligands attached to opposite sides of the metal cation, a configuration that reduces ligand−ligand repulsion.[8,34]

5. Conclusions

The main outcomes of this work can be summarized as follows:

(1) Rotationally resolved IR spectra are obtained for Mg^+-H_2 and Mg^+-D_2 in the H−H and D−D stretch regions, respectively. Band centers for the ν_{HH} and ν_{DD} transitions of Mg^+-H_2 and Mg^+-D_2 are red-shifted by 106.2 and 76.0 cm^{-1}, respectively, from the stretch fundamentals of the free H_2 and D_2 molecules.

(2) The Mg^+-H_2 complex has a T-shaped equilibrium structure with a vibrationally averaged $Mg^+\cdots H_2$ separation of 2.716 Å, decreasing by 0.037 Å when the H_2 subunit is vibrationally excited. The Mg^+-D_2 complex has a similar vibrationally averaged intermolecular separation (2.687 Å), which decreases upon D_2 vibrational excitation by 0.026 Å.

3. Lower limits for the predissociation lifetimes, estimated from the transition line widths, are 120 and 180 ps for Mg^+-H_2 and Mg^+-D_2, respectively.

It is clear that there is no simple, general relationship between vibrational red-shift and binding energy for the M^+-H_2 complexes, although periodic trends are beginning to emerge. Apparently, a complex containing a metal cation with a half-filled or filled valence s orbital has a larger ν_{HH} red-shift than a complex containing an alkali metal cation with a comparable dissociation energy.

Ultimately, a more comprehensive understanding of the floppy Mg^+-H_2 complex should be obtainable by calculating a full three-dimensional PES and using this to compute rovibrational energies that can be compared directly with spectroscopic transition energies. These calculations should also give reliable estimates for the dissociation energy and frequencies for the intermolecular vibrational modes.

Acknowledgment. The authors are grateful to the Australian Research Council for financial support.

Supporting Information Available: Transition wavenumbers and assignments. This material is available free of charge via the Internet at http://pubs.acs.org.

References and Notes

(1) Duncan, M. A. *Annu. Rev. Phys. Chem.* **1997**, *48*, 69–93.
(2) Ding, L. N.; Young, M. A.; Kleiber, P. D.; Stwalley, W. C.; Lyyra, A. M. *J. Phys. Chem.* **1993**, *97*, 2181–2185.
(3) Cheng, Y. C.; Chen, J.; Ding, L. N.; Wong, T. H.; Kleiber, P. D.; Liu, D. K. *J. Chem. Phys.* **1996**, *104*, 6452–6459.
(4) Kleiber, P. D.; Lu, W.; Abate, Y. *Int. J. Mass Spectrom.* **2008**, *269*, 1–11.
(5) Guo, W.; Liu, H.; Yang, S. *Int. J. Mass Spectrom.* **2003**, *226*, 291–304.
(6) Walker, N. R.; Walters, R. S.; Tsai, M. K.; Jordan, K. D.; Duncan, M. A. *J. Phys. Chem. A* **2005**, *109*, 7057–7067.

(7) Thompson, C.; Emmeluth, C.; Poad, B.; Weddle, G.; Bieske, E. *J. Chem. Phys.* **2006**, *125*, 044310-5.
(8) Emmeluth, C.; Poad, B. L. J.; Thompson, C. D.; Weddle, G. H.; Bieske, E. J. *J. Chem. Phys.* **2007**, *126*, 204309.
(9) Emmeluth, C.; Poad, B. L. J.; Thompson, C. D.; Weddle, G. H.; Bieske, E. J.; Buchachenko, A. A.; Grinev, T. A.; Kłos, J. *J. Chem. Phys.* **2007**, *127*, 164310.
(10) Dryza, V.; Poad, B. L. J.; Bieske, E. J. *J. Am. Chem. Soc.* **2008**, *130*, 12986–12991.
(11) Poad, B. L. J.; Wearne, P. J.; Bieske, E. J.; Buchachenko, A. A.; Bennett, D.; Kłos, J.; Alexander, M. H. *J. Chem. Phys.* **2008**, *129,* 184306.
(12) Orimo, S.; Nakamori, Y.; Eliseo, J.; Zuttel, A.; Jensen, C. *Chem. Rev.* **2007**, *107*, 4111–4132.
(13) Sakintuna, B.; Lamari-Darkrim, F.; Hirscher, M. *Int. J. Hydrogen Energy* **2007**, *32*, 1121–1140.
(14) Han, S. S.; Deng, W. Q.; Goddard, W. A. *Angew. Chem., Int. Ed.* **2007**, *46*, 6289–6292.
(15) Dinca, M.; Long, J. R. *J. Am. Chem. Soc.* **2005**, *127*, 9376–9377.
(16) Arean, C. O.; Palomino, G. T.; Carayol, M. R. L. *Appl. Surf. Sci.* **2007**, *253*, 5701–5704.
(17) Torres, F. J.; Civalleri, B.; Terentyev, A.; Ugliengo, P.; Pisani, C. *J. Phys. Chem. C* **2007**, *111*, 1871–1873.
(18) Lochan, R. C.; Head-Gordon, M. *Phys. Chem. Chem. Phys.* **2006**, *8*, 1357–1370.
(19) Page, A. J.; von Nagy-Felsobuki, E. I. *Chem. Phys.* **2008**, *351*, 37–45.
(20) Kleiber, P. D.; Chen, J. *Int. Rev. Phys. Chem.* **1998**, *17*, 1–34.
(21) Staanum, P. F.; Højbjerre, K.; Wester, R.; Drewsen, M. *Phys. Rev. Lett.* **2008**, *100*, 243003.
(22) Petrie, S.; Dunbar, R. C. *J. Phys. Chem. A* **2000**, *104*, 4480–4488.
(23) Curtiss, L. A.; Pople, J. A. *J. Phys. Chem.* **1988**, *92*, 894–9.
(24) Bauschlicher, C. W. *Chem. Phys. Lett.* **1993**, *201*, 11–14.
(25) Frisch, M. J. et al. *Gaussian 03*, revision.01; Gaussian Inc.: Wallingford, CT, 2004. The full reference is given in the Supporting Information.
(26) Lovejoy, C.; Nelson, D.; Nesbitt, D. J. *J. Chem. Phys.* **1987**, *87*, 5621–5628.
(27) Bieske, E. J.; Nizkorodov, S. A.; Bennett, F. R.; Maier, J. P. *J. Chem. Phys.* **1995**, *102*, 5152–64.
(28) Huber, K. P.; Herzberg, G. *Molecular Spectra and Molecular Structure IV. Constants of Diatomic Molecules*; van Nostrand Reinhold: New York, 1979.
(29) Bragg, S. L.; Brault, J. W.; Smith, W. H. *Astrophys. J.* **1982**, *263*, 999–1004.
(30) Bauschlicher, C. W. *Chem. Phys. Lett.* **1993**, *201*, 11–14.
(31) Nesbitt, D. J.; Naaman, R. *J. Chem. Phys.* **1989**, *91*, 3801.
(32) Wild, D. A.; Weiser, P. S.; Bieske, E. J. *J. Chem. Phys.* **2001**, *115*, 6394–6400.
(33) Wild, D. A.; Bieske, E. J. *J. Chem. Phys.* **2004**, *121*, 12276–12281.
(34) Bauschlicher, C. W., Jr.; Partridge, H.; Langhoff, S. R. *J. Phys. Chem.* **1992**, *96*, 2475–2479.
(35) Bushnell, J. E.; Kemper, P. R.; Bowers, M. T. *J. Phys. Chem.* **1994**, *98*, 2044–2049.
(36) Kemper, P. R.; Bushnell, J.; Bowers, M. T.; Gellene, G. I. *J. Phys. Chem.* **1998**, *102*, 8590–8597.
(37) Kemper, P. R.; Bushnell, J. E.; Weis, P.; Bowers, M. T. *J. Am. Chem. Soc.* **1998**, *120*, 7577.
(38) Olkhov, R. V.; Nizkorodov, S. A.; Dopfer, O. *J. Chem. Phys.* **1997**, *107*, 8229–8238.
(39) Vitillo, J. G.; Damin, A.; Zecchina, A.; Ricchiardi, G. *J. Chem. Phys.* **2005**, *122*, 114311/1–114311/10.
(40) Kraemer, W. P.; Špirko, V. *Chem. Phys.* **2006**, *330*, 190–203.
(41) Sharp, S. B.; Gellene, G. I. *J. Am. Chem. Soc.* **1998**, *120*, 7585.

JP808807R